Journal of Electronic Materials (2022) 51:6388–6396
https://doi.org/10.1007/s11664-022-09872-5

ORIGINAL RESEARCH ARTICLE

A Novel HM-HD-RFET Biosensor for Label-Free Biomolecule Detection

Arpita Biswas[1] · Chithraja Rajan[2] · Dip Prakash Samajdar[3]

Received: 11 September 2021 / Accepted: 5 August 2022 / Published online: 2 September 2022

Abstract

The mortality of people worldwide caused by COVID-19 has enhanced the research interest to design and develop power-efficient, low-cost, and sensitive biosensors to detect a wide range of biomolecules or foreign particles that can cause severe negative impact on humans. A novel Bio-RFET biosensor with hetero-material (HM) for source/channel and drain regions and hetero-dielectric (HD) is proposed, which acts as an *n*-MOSFET or a *p*-MOSFET and *n*-TFET or *p*-TFET. This HM-HD-RFET biosensor senses the biomolecules by the label-free dielectric modulation (DM) technique. When the biomolecules are present in the nanocavity, the biosensor can detect the biomolecules without labeling costs. It also changes the dielectric polarization within the nanocavities, and causes a drain current variation in the presence of an electric field. In this research article, ($SiO_2 + TiO_2$) and an AlGaAs/Ge-based HD-HM-RFET have been analyzed for their use in biosensing. We found that the proposed device exhibits higher sensitivity as compared to a $SiO_2 + HfO_2$-HM-RFET and a Si-based $SiO_2 + TiO_2$-RFET for varying dielectric constants (K) from $K = 20$–80 and charge densities in the range -5×10^{11} to 1×10^{13} C/cm^2. Further, it can be noticed that *n*-$SiO_2 + TiO_2$-HM-TFET possesses the highest I_d-V_{gs} sensitivity of 5.09×10^{13}, I_{ON}/I_{OFF} ratio of 1.23×10^9, lowest SS of 20.3 mV/dec, and V_{th} of 1.48 V.

Keywords TFET · Biosensor · Hetero material (HM) · Hetero dielectric (HD) · Dielectric modulation (DM) · Sensitivity

Introduction

Infection-specific biosensors need detailed analysis and research, which increases the time for disease detection and recovery rate. Labeling is another major limitation of biosensors, as marking them with defect-specific materials is a cost-consuming procedure.[1] These limitations are mostly suppressed in dielectric modulated (DM) label-free FET-based biosensors that efficiently detect a wide variety of biomolecules, and, hence, are extremely helpful for the biomedical industry.[2] Therefore, in this work, we have investigated a novel hetero-material (HM) hetero-dielectric (HD) reconfigurable FET (RFET) biosensor, which detects a wide variety of neutral and charged biomolecules by label-free detection methods.[3–5]

RFET is an electrically doped (ED) junctionless device, such that an oversource and drain electrodes attract electrons/holes depending on the polarity (positive/negative) of the applied potential.[6] Further, RFET behaves as either a MOSFET or a TFET as compared to a physically doped (PD) device.[7,8] However, a Si-RFET has some limitations, like high ambipolarity and low ON current of the TFET and high OFF current of the MOSFET.[9–11] MOSFET-based biosensors are inferior in terms of biomolecule detection and power consumption, as compared to TFET-based biosensors exhibiting lower OFF current and lower subthreshold swing (< 60 mV/dec).[12–15] However, MOSFET-based biosensors produce more ON current and are useful in the circuitry. Here, using the HD oxide layer ($SiO_2 + TiO_2$) and the HM AlGaAs/Ge, we upgrade the characteristics of both MOSFET and TFET-based biosensors. Further, on comparing the proposed biosensor with a Si-HD-RFET biosensor, we

✉ Dip Prakash Samajdar
dipprakash010@gmail.com

Arpita Biswas
arpitabiswas18919@gmail.com

Chithraja Rajan
rajan.chithraja@gmail.com

1 Department of Electrical Engineering, Indian Institute of Technology Jodhpur, Jodhpur, Rajasthan, India

2 Shri Ramdeobaba College of Engineering and Management, Nagpur, Maharashtra, India

3 PDPM Indian Institute of Information Technology, Design and Manufacturing, Jabalpur, Madhya Pradesh, India

found that the new device excels in its sensing ability and reconfigurability.

Some typical examples of biomolecules, with the range of their K values given in parentheses, include SARS-CoV-2 (1–4), Uriease (1.64), Streptavidin (2.1), GOx (3.46), 3-aminopropyltriethoxysilane (APTES) (3.57), Ferro-cytochrome c (4.7), RNA converted to C-DNA (1—64), etc.[16,17].

HD-HM-RFET-Based Biosensor

Device Configuration and Simulation Details

The structures of HM-HD-RFET- and Si-HD-RFET-based biosensors are depicted in Figs. 1 and 2, respectively. The heterostructure combination of high band gap AlGaAs in the source/channel region and the low band gap Ge in the drain improves the ON current of the proposed device. While high-K dielectric TiO_2 near the source/channel junction is used to further boost the ON current, low-K dielectric SiO_2 reduces the ambipolarity.[18] The substrate doping concentration is taken to be 10^{15} cm^{-3}.

Here, the ED mechanism is used to permit a reconfigurable nature of the biosensor, and is used to overcome the limitation of the PD mechanism, like random dopant fluctuation.[19,20] Potentials $\pm$ 1.2 V are applied to the overdrain (V_{ODS}) and the oversource (V_{OSS}) electrodes to allow the reconfigurable nature of the device, and it behaves as *n*- or *p*-type MOSFET or TFET-based biosensor.[21–23] The *n*-MOSFET-based biosensor ($Voss$ = 1.2 V and V_{ODS} = 1.2 V), *p*-MOSFET-based biosensor (V_{OSS} = − 1.2 V and V_{ODS} = − 1.2 V), *n*-TFET-based biosensor (V_{OSS} = − 1.2 V and V_{ODS} = 1.2 V) and *p*-TFET-based biosensor (V_{OSS} = 1.2 V and V_{ODS} = − 1.2 V) are four different configurations discussed here. Two nanocavities are built below the gate electrode where the biosensor introduces the biomolecules. Dimensions of the devices are listed in Table I.

In this work, we have used one of the powerful physically based simulation through the Silvaco Atlas tool that provides insight physics of two- and three-dimensional semiconductor devices by accommodating various physical and mathematical models.[24] Atlas simulations use two types of input file, a structure file and a command file. The structure and command files refer to the structure to be simulated, and the list of instructions needed to simulate it. In addition, there are three types of output files, runtime, log file, and solution file. The runtime file demonstrate errors alarming comments during the live simulation. The log file contains voltages and the current defined at all the nodes, while the

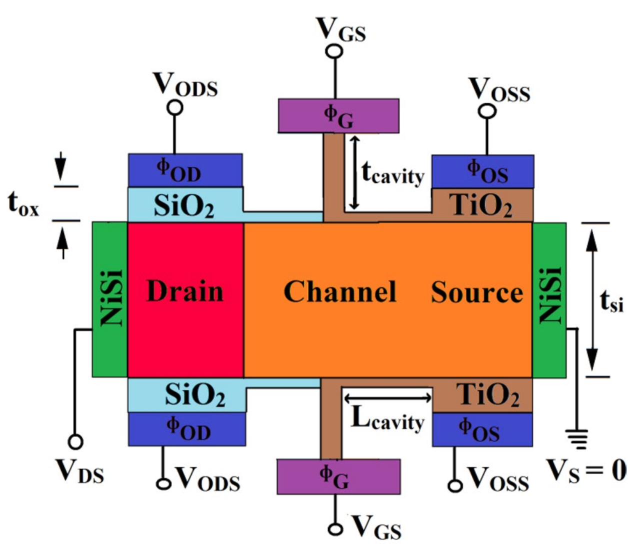

Fig. 1 HM-HD-RFET biosensor structure.

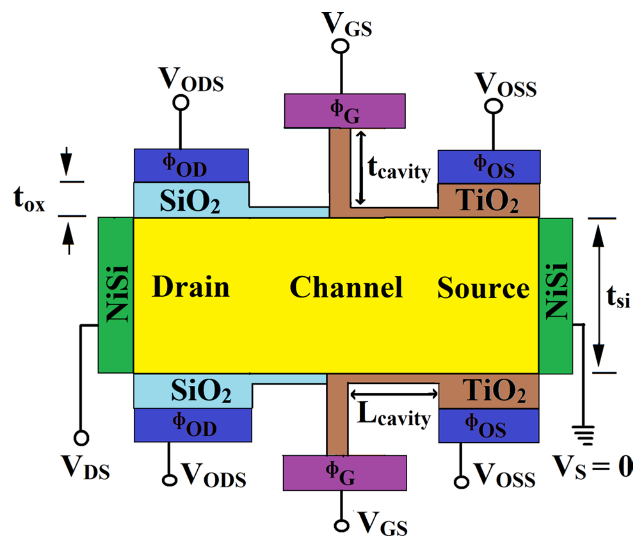

Fig. 2 Si-HD-RFET biosensor structure.

Table I Design parameters HM-HD-RFET-based biosensor

Parameter name and unit	Symbol	HM-HD-RFET
Overdrive source length (nm)	L_{OS}	50
Overdrive drain length (nm)	L_{OD}	50
Gate to source/drain spacer length (nm)	L_{GS}/L_{GD}	5
Source/drain length (nm)	L_S/L_D	55
Gate length (nm)	L_G	50
Work function of overdrive source/drain (eV)	$\phi_{OS}/\ \phi_{OD}$	4.5
Gate metal work function (eV)	ϕ_G	4.7
Thickness of Si substrate (nm)	t_{si}	10
Gate oxide (SiO_2/TiO_2) thickness (nm)	t_{ox}	2
Length of cavity (nm)	L_{Cavity}	27.5
Thickness of cavity (nm)	t_{Cavity}	5.5

complete set data of all the solution variables are collectively presented in the solution file. The models used for the simulation of our proposed device are the Auger model, the Shockley–Read–Hall model Universal Schottky Tunneling model, Fermi Dirac Statistics and Klaassen's Unified Low Field Mobility models, bandgap narrowing model, non-local band-to-band tunneling model. All the models are calibrated with the experimental data for validation. Figure 3 shows the close matching of the experimental[10] and simulated data.

Operation of HM-HD-RFET-Based Biosensor for Different Values of K

In the four different configurations, the drain current variation of the HM-HD-RFET biosensor is shown in Fig. 4 for different K values (1, 20, 40, 60, and 80) of neutral biomolecules. Figure 4a shows that, with the increase in K value, the driving current of the p-HM-HD-MOSFET biosensor also increases while there is little improvement in the case of n-HM-HD-MOSFET. In Fig. 4b, the drain current (I_d) of the p-HM-HD-TFET and n-HM-HD TFET biosensors also increases with K.

The variation of energy band diagram (EBD) and surface potential is shown in Fig. 4c, d for n-HM-HD-RFET and the explanation of EBD and surface potential for the p-type device is skipped to avoid redundancy. In the n-HM-HD-MOSFET, the energy band in the channel region bends downwards further as the K value increases (Fig. 4c). Because of the band bending, the drain current and the surface potential are enhanced (Fig. 4d). Thus, all the four FETs-based biosensors offer better sensing ability for different types of biomolecules.

Operation of HM-HD-RFET-Based Biosensor for Biomolecules with Different Charge Densities

Figure 5 shows the I_d variation of the HM-HD-RFET-based biosensor in four different configurations for positively and negatively charged biomolecules, keeping K fixed at 80. Figure 5a shows that, with the increase in the positive charge density, I_d increases for the n-HM-HD-MOSFET but decreases for the p-HM-HD-MOSFET in the linear region. Note that the threshold voltage (V_{th}) decreases for the n-HM-HD-MOSFET, while it increases for the p-HM-HD-MOSFET. Figure 5b shows a similar effect on the HM-HD-TFET-based biosensor. Exactly opposite characteristics can be observed with the rise in negative charge densities, as shown in Fig. 5c, d, where, with the increase in the negative charge of the biomolecules, I_d decreases for the n-type and increases for the p-type devices in the linear region, while the reverse scenario is observed for V_{th}.

HM-HD-RFET and Si-HD-RFET Based Biosensors

This section compares the HM-HD-RFET-based biosensor with the Si-HD-RFET-based biosensor to evaluate the importance of using III–V semiconductors in label-free biosensing applications. We compared the variation of I_d of the HM-HD-RFET- and Si-HD-RFET-based biosensors for the idle situation ($K = 1$) and for the charge 1×10^{13} C/cm^2 and $K = 80$. Figure 6a shows that the I_d of the Si-HD-MOSFET-based biosensor is higher than that of the HM-HD-MOSFET-based biosensor, both in the absence and presence of the biomolecules. However, our device gives a lower I_d as compared to the Si-based biosensor, which indicates that the HM-HD-MOSFET is less sensitive towards ($K = 1$) air, and that it consumes less power for the idle situation.

Figure 6b shows that the EBD of Si-HD-MOSFET-based biosensor is flatter for the absence and presence of the biomolecules when compared to the HM-HD-MOSFET-based biosensor, because high band gap material is present in the channel region. Therefore, the Si-HD-MOSFET-based biosensor provides better I_d than the HM-HD-MOSFET-based biosensor. Similarly, I_d of the proposed and Si TFET-based biosensors are compared at $K = 80$ and charge = 1×10^{13} C/cm^2, and $K = 1$ in Fig. 6c. Here, we noticed that the I_d of the HM-HD-TFET-based biosensor is lower than that of the Si-HD-TFET-based biosensor, which indicates that the HM-HD-TFET is less sensitive towards the ($K = 1$) air when compared to the Si-HD-TFET, and, hence, a lower power consumption and better sensitivity can be observed for this device. Again, the EBD of the proposed and Si-based devices in Fig. 6d shows that the band bending of the HM-HD-TFET device is less steep than for the Si device due to the band gap difference at the tunneling junction.

Sensitivity Comparison

$I_d{-}V_{gs}$ sensitivity of the bio-FET-based biosensor has been obtained from Eq. 1, showing that the $I_d{-}V_{gs}$ sensitivity is the ratio of the difference in I_d in the absence ($K = 1$) and the presence of the biomolecules (K > 1) to that of I_d in the idle condition ($K = 1$):

$$S_{Id} = \left(I_d^{Bio} - I_d^{Air}\right) / I_d^{Air} \tag{1}$$

where, S_{Id} is the I_d-V_{gs} sensitivity of the bio-FET-based biosensor, I_d^{Air} is the drain current obtained in the absence of the biomolecules, and I_d^{Bio} is the drain current when the biomolecules are present in the nanocavity.

Figure 7 compares the maximum $I_d{-}V_{gs}$ sensitivity of the two devices for different K of the biomolecules. Note that the proposed device behaves as a better bio-RFET-based biosensor as compared to the Si-HD-RFET-based biosensor for different K. Also, for both the HM-HD-RFET and Si-HD-RFET devices, TFET-based biosensors provide better I_d–V_{gs} sensitivity than MOSFET-based biosensors when K is varied in the range from 20 to 80. *p*-MOSFET-based biosensors outperforms *n*-MOSFET-based biosensors for both cases. However, both *n*-TFETs and *p*-TFETs are superior to *n*-MOSFETs and *p*-MOSFETs, and offer the same sensing capability. The introduction of the high band gap AlGaAs in the channel and source regions is the prime factor for the improvement of the I_d-V_{gs} sensitivity of all the four FET characteristics.

Similarly, Figs. 8 and 9 compare the maximum I_d–V_{gs} sensitivity of the HM-HD-RFET and Si-HD-RFET-based biosensor for the different positively and negatively charged biomolecules. From the different charge values, it is clear that the HM-HD-RFET-based device is a better bio-RFET biosensor as compared to the Si-HD-RFET-based device. Also, it can be seen that TFET-based devices provide better I_d–V_{gs} sensitivity as compared to MOSFET-based devices when charge values are increased, irrespective of sign. In other words, the device sensitivity I_d–V_{gs} increases as the negative charge value decreases or the positive charge value increases. The *p*-MOSFET-based biosensors sense charged biomolecules better than the *n*-MOSFET-based biosensor for both the two cases.

However, both *n*-TFET and *p*-TFET devices are superior to *n*-MOSFET and *p*-MOSFET devices and offer the same sensing capability. Here, we observed that the HM combination and the oxide layer with higher dielectric constant are favorable for biosensing applications.

Table II compares the sensitivity of the proposed RFET biosensor with the others available in the literature and it is found that *n*-HM-HD-TFET provides better sensitivity. Further, Fig. 10 shows that as the biomolecule occupancy in the cavity reduces from full (100%) to one-quarter (25%) of total area, the sensing capability decreases to 38.4% for half of the occupancy and 85.1% for one-quarter of the occupancy. Therefore, we found that steric hindrance[34] is a major issue in nanoscale biosensors as it reduces the biosensor performance to a considerable extent. The phenomenon of steric hindrance is analyzed in details in Ref. 35 and 36.

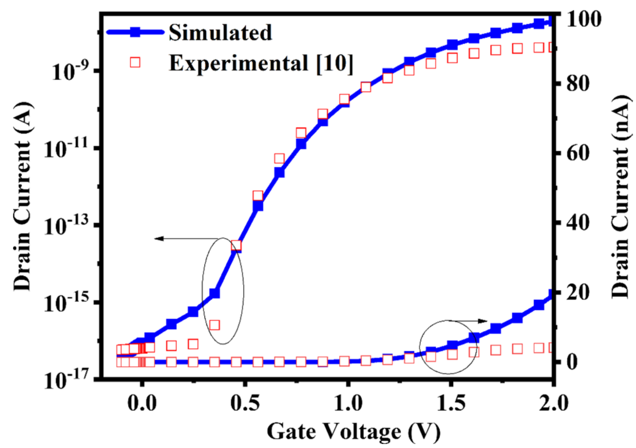

Fig. 3 Calibration with experimental results.

Table II Comparison between various biosensors available in the literature with the proposed work

Biosensors	L_{cavity} (nm)	t_{cavity} (nm)	k	Current sensitivity
JL-DM-ED-TFET[25]	10	5	10	6.89×10^5
CP-DM-JL-TFET[17]	23	5.5	10	1.08×10^8
CP-DM-GU-JLTFET[25]	23	5.5	10	1.16×10^4
CG-TFET[26]	25	11	10	2.32×10^7
DMDG TFET[27]	150	9	10	4.82×10^7
HM-SE-TFET[14]	30	5.5	5	4.1×10^4
DG-TFET[28]	23	5.5	5	0.66×10^3
DM-LTFET[29]	45	5	17	2150
SG-Si-NT-FET[30]	15	10	20	2
DMG-DC-CP-TFET[16]	20	5.5	12	8.7×10^{10}
SC-DM-EG HTFET[11]	30	5	12	1.7×10^8
DM-DSTGTFET[31]	37	5	23	1.38×10^5
JL-TFET[32]	20	–	9	16.85
Bio-NT-TFET[33]	10	2	20	100
HM-HD-*n*-MOSFET (this work)	27.5	5.5	20	9113.06
HM-HD-*p*-MOSFET (this work)	27.5	5.5	20	1.74×10^7
HM-HD-*n*-TFET (this work)	27.5	5.5	20	1.32×10^{13}
HM-HD-*p*-TFET (this work)	27.5	5.5	20	8.42×10^{10}

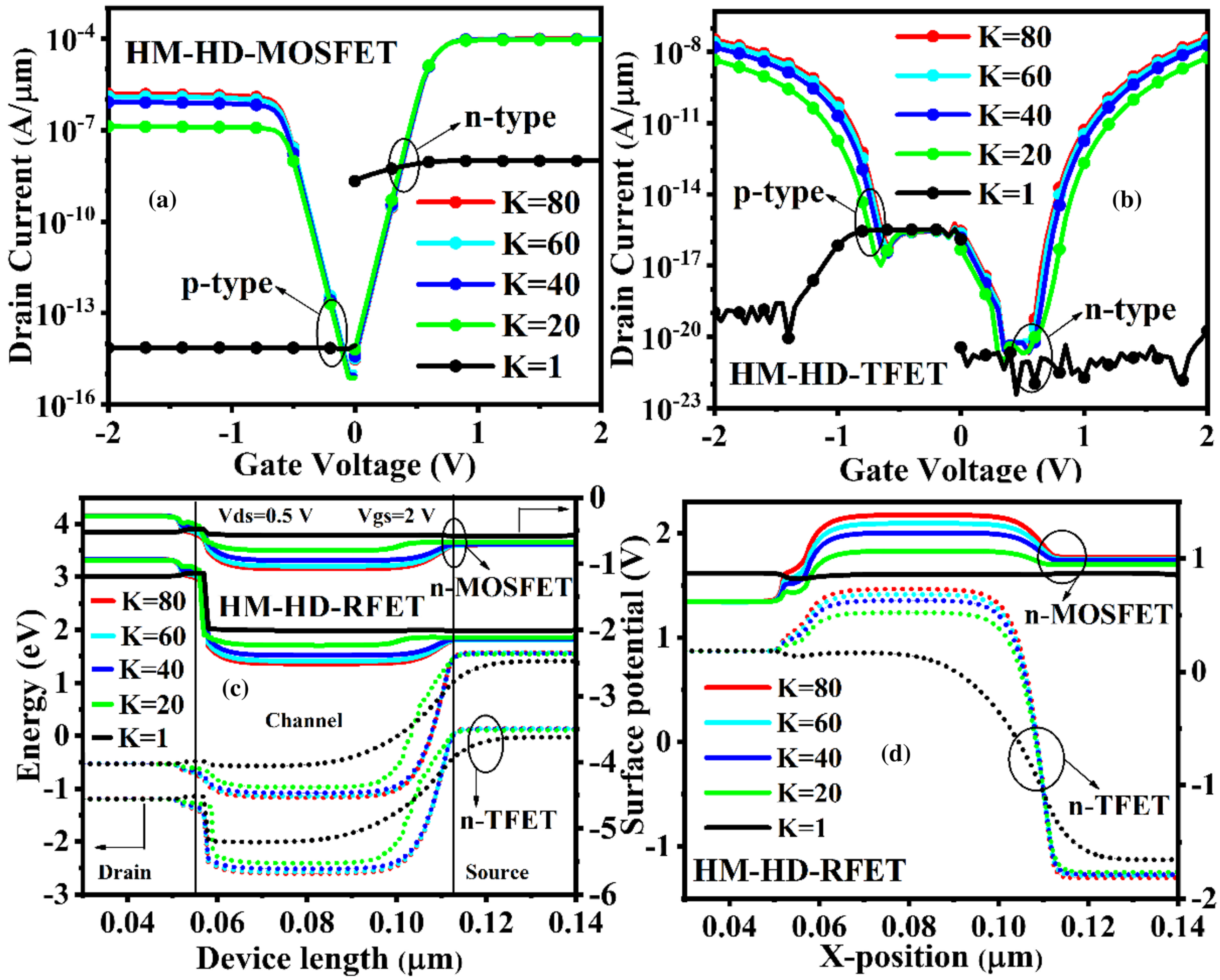

Fig. 4 I_d-V_{gs} characteristics of (a) HM-HD-MOSFET, (b) HM-HD-TFET, and (c) energy band diagram (EBD), (d) surface potential of the HM-HD-RFET biosensor for different K.

Conclusions

A unique HM-HD-RFET-based biosensor is proposed and investigated to evaluate its potential to sense the biomolecules through the use of HD (SiO_2 + TiO_2) beneath the gate and HM (AlGaAs/Ge) in the source/channel and drain regions. RFET-based devices function either as *n*-MOSFET or *p*-MOSFET and *n*-TFET or *p*-TFET. Hence, four different configurations of FET-based biosensors are possible with a single device. Here, we explored the four configurations to produce a biosensor that can detect a wide range of biomolecules by introducing a cavity in the device. However, the Si-HD-TFET biosensor does not provide enough ON current. The designed bio-RFET sensor is compared with its Si-HD-RFET counterpart for the detection of biomolecules with different K values (0–80) and charge densities (-5×10^{11} to 1×10^{13} C/cm^2). It can be concluded from the results that the HM-HD-RFET exhibits a better sensitivity than the Si-HD-RFET-based biosensor.

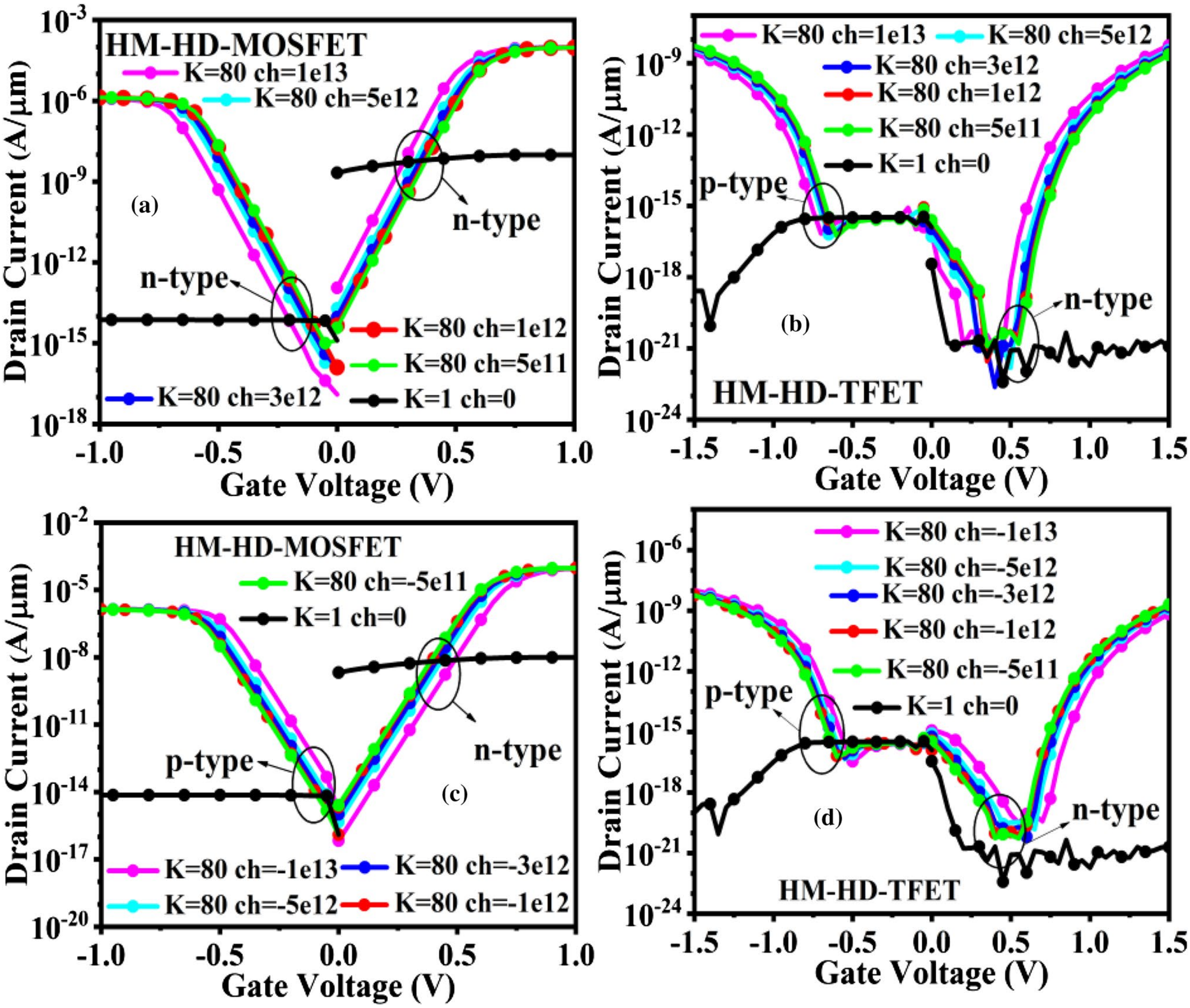

Fig. 5 I_d-V_{gs} characteristics of (a) HM-HD-MOSFET, (b) HM-HD-TFET for positive charge density, and (c) HM-HD-MOSFET, and (d) HM-HD-TFET biosensors for different negative charge densities.

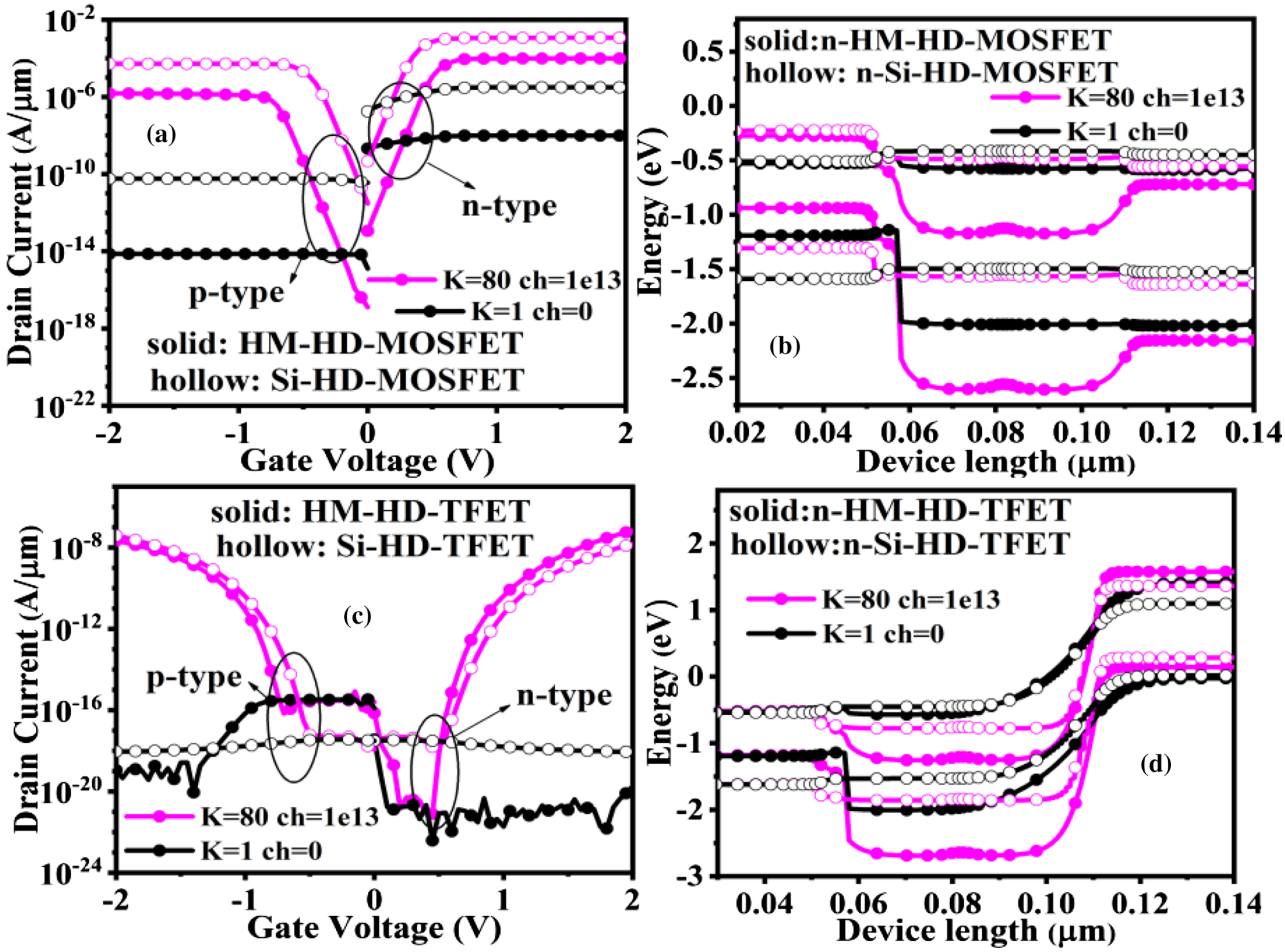

Fig. 6 (a) I_d-V_{gs} plots and (b) EBD in between HM-HD-MOSFET abdSi-HD-MOSFET and (c) I_d-V_{gs} plots (d) EBD in between HM-HD-TFET and Si-HD-TFET biosensors.

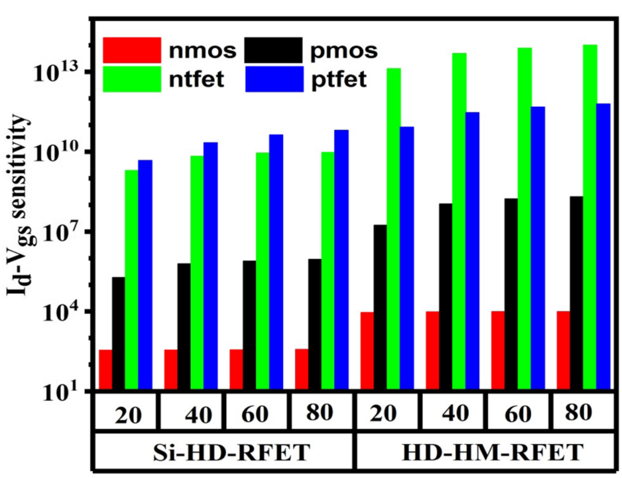

Fig. 7 I_d-V_{gs} sensitivity of HM-HD-RFET and Si-HD-RFET biosensors for different K.

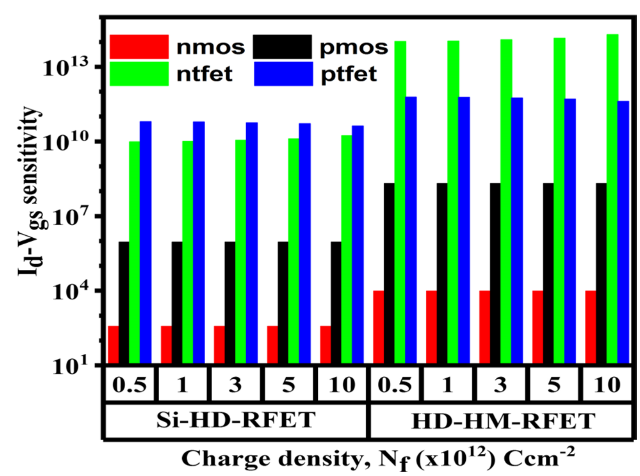

Fig. 8 I_d-V_{gs} sensitivity of HM-HD-RFET and Si-HD-RFET-based biosensors for positive charge densities.

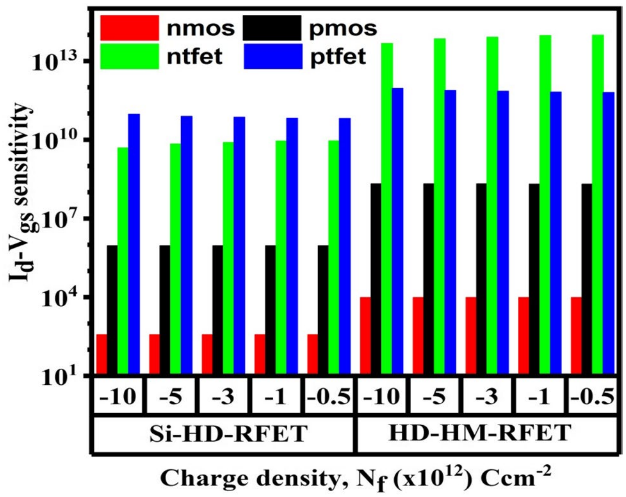

Fig. 9 I_d-V_{gs} sensitivity value of HM-HD-RFET and Si-HD-RFET-based biosensors for negative charge densities.

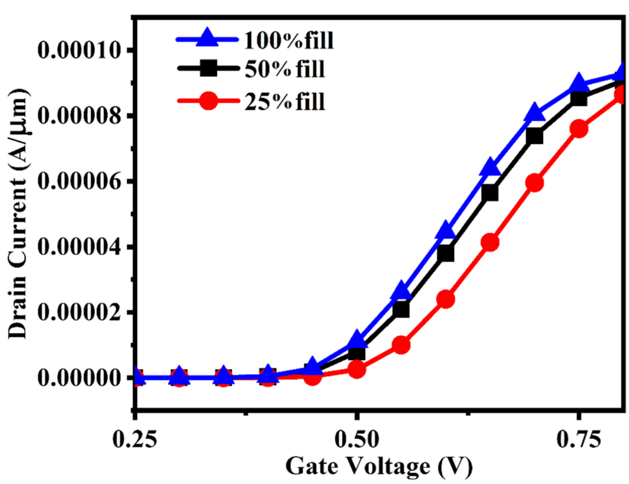

Fig. 10 The impact of steric hindrance on biosensor performance.

Conflict of interest The authors declare that they have no conflict of interest.

References

1. C. Drosten, S. Drosten, W. Preiser, S.V.D. Werf, H.R. Brodt, S. Becker, H. Rabenau et al., Identification of a Novel Coronavirus in Patients with Severe Acute Respiratory Syndrome. *New England J. Med.* 348, 1967–1976 (2003). https://doi.org/10.1056/NEJMoa030747.
2. A.M. Zaki, S.V. Boheemen, T.M. Bestebroer, A.D.M.E. Osterhau, and R.A.M. Fouchier, Isolation of a Novel Coronavirus from a Man with Pneumonia in Saudi Arabia. *New England J Med.* 367, 1814 (2012). https://doi.org/10.1056/NEJMoa1211721.
3. S. Yadav, A. Gedam, and S. Tirkey, A Dielectric Modulated Biosensor for SARS-CoV-2. *IEEE Sensors J.* 21, 14483 (2020). https://doi.org/10.1109/JSEN.2020.3019036.
4. J.F.-W. Chan, S. Yuan, K.-H. Kok, K.K.-W. To, H. Chu, J. Yang et al., A Familial Cluster of Pneumonia Associated with the 2019 Novel Coronavirus Indicating Person-to-Person Transmission: A Study of a Family Cluster. *Lancet* 395, 514 (2020). https://doi.org/10.1016/S0140-6736(20)30154-9.
5. K. Priyadarshi, V.L. Nag, S.P. Kombade, R.S. Gadepalli, S. Misra, and K. Singh, Molecular Diagnosis of COVID-19: An Update and Review. *Ann. Natl. Acad. Med. Sci. (India)* 3, 126–137 (2020). https://doi.org/10.1055/s-0040-1713836.
6. S. Kalra, M.J. Kumar, and A. Dhawan, Reconfigurable FET Biosensor for a Wide Detection Range and Electrostatically Tunable Sensing Response. *IEEE Sens. J.* 20, 2261 (2019). https://doi.org/10.1109/JSEN.2019.2952333.
7. A. Biswas, C. Rajan, and D.P. Samajdar, A Novel RFET Sensor for Label-Free Biomolecule Detection. *Silicon* (2022). https://doi.org/10.1007/s12633-022-01683-x.
8. C. Rajan and D.P. Samajdar, Design Principles for a Novel Lightweight Configurable PUF Using a Reconfigurable FET. *IEEE Trans. Electron Dev.* 67, 5797 (2020). https://doi.org/10.1109/TED.2020.3030868.
9. P. Saha, D.K. Dash, and S.K. Sarkar, Nanowire Reconfigurable FET as Biosensor: Based on Dielectric Modulation Approach. *Solid-State Electron.* 161, 107637 (2019). https://doi.org/10.1016/j.sse.2019.107637.
10. H. Im, X.J. Huang, B. Gu, and Y.K. Choi, A Dielectric Modulated Field-Effect Transistor for Biosensing. *Nat. Nanotechnol.* 2, 430 (2007). https://doi.org/10.1038/nnano.2007.180.
11. S. Mukhopadhyay, D. Sen, B. Goswami, and S.K. Sarkar, Performance Evaluation of Dielectrically Modulated Extended Gate Single cavity InGaAs/Si HTFET Based Label-Free Biosensor Considering Non-ideal Issues. *IEEE Sens. J.* 21, 4739 (2020). https://doi.org/10.1109/JSEN.2020.3033576.
12. A. Biswas, C. Rajan, and D.P. Samajdar, Sensitivity Analysis of Physically Doped, Charge Plasma and Electrically Doped TFET Biosensors. *Silicon* (2021). https://doi.org/10.1007/s12633-021-01461-1.
13. S.K. Agnihotri, D.P. Samajdar, C. Rajan, A.S. Yadav, and G. Gnanesh, Performance analysis of gate engineered dielectrically modulated TFET biosensors. *Int. J. Electron.* 108, 607 (2020). https://doi.org/10.1080/00207217.2020.1793407.
14. A. Lodhi, C. Rajan, A.K. Behera, D.P. Samajdar, D. Soni, and D.S. Yadav, Sensitivity and Sensing Speed Analysis of Extended Nano-Cavity and Source Over Electrode in Si/SiGe Based TFET Biosensor. *Appl. Phys. A* 126, 1 (2020). https://doi.org/10.1007/s00339-020-04008-0.
15. D. Soni and D. Sharma, Design of NW TFET Biosensor for Enhanced Sensitivity and Sensing Speed by Using Cavity Extension and Additional Source Electrode. *Micro. Nano Lett.* 14, 901 (2019). https://doi.org/10.1049/mnl.2018.5733.
16. M. Mahalaxmi, B. Acharya, and G.P. Mishra, Design and Analysis of Dual-Metal-Gate Double-Cavity Charge-Plasma-TFET as a Label Free Biosensor. *IEEE Sensors J.* 20, 13969 (2020). https://doi.org/10.1109/JSEN.2020.2979016.
17. D. Singh, S. Pandey, K. Nigam, D. Sharma, D.S. Yadav, and P. Kondekar, A Charge-Plasma-Based Dielectric-Modulated Junctionless TFET for Biosensor Label-Free Detection. *IEEE Trans. Electron Dev.* 64, 271 (2016). https://doi.org/10.1109/TED.2016.2622403.
18. K. Boucart and A.M. Ionescu, Double-Gate Tunnel FET with High-k Gate Dielectric. *IEEE Trans. Electron Dev.* 54, 1725 (2007). https://doi.org/10.1109/TED.2007.899389.
19. S. Yadav, R. Madhukar, D. Sharma, M. Aslam, D. Soni, and N. Sharma, A New Structure of Electrically Doped TFET for

Improving Electronic Characteristics. *Appl. Phys. A* 124, 517 (2018). https://doi.org/10.1007/s00339-018-1930-9.
20. D. Sharma, D. Singh, S. Pandey, S. Yadav, and P.N. Kondekar, Comparative Analysis of Full-Gate and Short-Gate Dielectric Modulated Electrically Doped TunNel-FET Based Biosensors. *Superlattices Microstruct.* 111, 767 (2017). https://doi.org/10.1016/j.spmi.2017.07.035.
21. H. Latikhameneh, T.A. Ameen, G. Klimeck, J. Appenzeller, and R. Rahman, Dielectric Engineered Tunnel Field-Effect Transistor. *IEEE Electron Dev. Lett.* 36, 1097 (2015). https://doi.org/10.1109/LED.2015.2474147.
22. B.V. Chandan, K. Nigam, C. Rajan, and D. Sharma, A Fair Comparison of the Performance of Charge Plasma and Electrostatic Tunnel FETs for Low-Power High-Frequency Applications. *J. Comput. Electron.* 18, 1201 (2019). https://doi.org/10.1007/s10825-019-01388-2.
23. B.R. Raad, S. Tirkey, D. Sharma, and P. Kondekar, A New Design Approach of Dopingless Tunnel FET for Enhancement of Device Characteristics. *IEEE Trans. Electron Dev.* 64, 1830 (2017). https://doi.org/10.1109/TED.2017.2672640.
24. ATLAS Device Simulation Software, Silvaco International, Santa Clara, CA, USA. Aug. (2016)
25. B. Venkata et al., Junctionless Based Dielectric Modulated Electrically Doped Tunnel FET Based Biosensor for Label-Free Detection. *Micro Nano Lett.* 13, 452 (2017).
26. G. Wadhwa and B. Raj, Label Free Detection of Biomolecules Using Charge-Plasma-Based Gate Underlap Dielectric Modulated Junctionless TFET. *J. Electron. Mater.* 47, 4683 (2018).
27. R. Goswami et al., Comparative Analysis of Circular Gate TFET and Heterojunction TFET for Dielectric-Modulated Label-Free Biosensing. *IEEE Sens. J.* 19, 9600 (2019).
28. S.L. Noor, M.Z. Khan, Application of nanocavity embedded dual metal double gate TFET in biomolecule detection, In Humanitarian Technology Conference (R10-HTC) IEEE Region, pp. 345–348 (2017)
29. N. Shafi, C. Sahu, C. Periasamy, J. Singh, SiGe source charge plasma TFET for biosensing applications, In Nanoelectronic and Information Systems (iNIS), 2017 IEEE International Symposium, pp. 93–98 (2017)
30. C. Chong, H. Liu, S. Wang, S. Chen, and H. Xie, Sensitivity Analysis of Biosensors Based on a Dielectric-Modulated L-Shaped Gate Field-Effect Transistor. *Micromachines* 12, 19 (2021). https://doi.org/10.3390/mi12010019.
31. A. Singh, S. Chaudhury, M. Chanda, and C.K. Sarkar, Split Gated Silicon Nanotube FET for Bio-Sensing Applications. *IET Circuits Dev. Syst.* 14, 1289 (2020). https://doi.org/10.1049/iet-cds.2020.0208.
32. C. Chong, H. Liu, S. Wang, and S. Chen, Simulation and Performance Analysis of Dielectric Modulated Dual Source Trench Gate TFET Biosensor. *Nanoscale Res. Lett.* 16, 1 (2021).
33. R.B. Peesa, and D.K. Panda, Rapid Detection of Biomolecules in a Junction Less Tunnel Field-Effect Transistor (JL-TFET) Biosensor. *Silicon* 14, 1705 (2022). https://doi.org/10.1007/s12633-021-00981-0.
34. A.K. Gupta and A. Raman, Design, Investigation, and Sensitivity Analysis of a Biosensor Based on an Optimized Electrostatically Doped Nanotube TFET. *J. Electron. Mater.* 50, 5462 (2021).
35. A. Bhattacharyya, M. Chanda, and D. De, Performance Assessment of New Dual-Pocket Vertical Heterostructure Tunnel FET-Based Biosensor Considering Steric Hindrance Issue. *IEEE Trans. Electron Dev.* 66, 3988 (2019).
36. J. Talukdar, G. Rawat, and K. Mummaneni, Dielectrically Modulated Single and Double Gate Tunnel FET Based Biosensors for Enhanced Sensitivity. *IEEE Sens. J.* 21, 26566 (2021).